Int. J. Heat Mass Transfer. Vol. 31, No. 2, pp. 259–265, 1988
Printed in Great Britain

0017–9310/88 $3.00 + 0.00

Dissimilarity between heat and momentum transfer in a turbulent boundary layer disturbed by a cylinder

H. SUZUKI, K. SUZUKI and T. SATO†
Department of Mechanical Engineering, Kyoto University, Kyoto 606, Japan

(*Received* 7 *September* 1987)

Abstract—The cause of the dissimilarity between heat and momentum transfer found in a flat plate boundary layer disturbed by a cylinder was studied from the viewpoint of a turbulent structure. It was concluded that the intensification of hot outward and cold wallward interactions incurred by the disturbance given by the cylinder is a major cause of dissimilarity.

INTRODUCTION

IT WAS reported in a previous paper [1] that heat transfer from a flat plate can be augmented by disturbing the turbulent boundary layer with a cylinder contrary to the resulting reduction in skin friction. This is an interesting fact not only from the viewpoint of heat transfer technology but also from a basic viewpoint. It would be important to study how this dissimilarity between the heat and momentum transfer comes about. Dissimilarity between the heat transfer and momentum transfer can result either from the dissimilarity in the mechanism of turbulent heat and momentum transfer or from the dissimilarity in the velocity and temperature profiles. Kawaguchi *et al.* [2] performed simultaneous measurements of the streamwise and normal components of velocity and temperature fluctuations in a turbulent boundary layer disturbed by a cylinder. They applied quadrant analysis to the measured turbulent signals and suggested that the outward and wallward interactions of the fluid motion could explain the dissimilarity between heat and momentum transfer in the disturbed boundary layer. Unfortunately, since they used an unheated cylinder, the dissimilarity found may have resulted simply from the dissimilarity of the boundary conditions between the velocity and temperature fields, which could lead to the dissimilarity between the velocity and temperature profiles. Therefore, the given discussion was not affirmative.

In the present study, the cylinder temperature was held at the same temperature as the wall surface just under the heated cylinder. By this arrangement, the boundary conditions between the velocity and temperature fields were similar. Therefore, which of the two possible causes mentioned above is a major one can possibly be identified if the present results are compared with the previous ones.

EXPERIMENTAL APPARATUS AND PROCEDURE

Because the experimental apparatus used in the present study was basically the same as used in the previous studies [1, 2], only an outline of the experimental apparatus is described here.

Figure 1 shows a schematic view of the wind tunnel used in the present study. The boundary layer developed on the floor upstream of the flat plate is drawn underneath the plate by an auxiliary blower (11). This established cross-sectional uniformity of the flow at the leading edge of the flat plate. Streamwise variation of the static pressure was minimized by changing the slope of the ceiling (5) of the wind tunnel. The magnitude of pressure non-uniformity was kept within $\pm 1\%$ of the main stream dynamic pressure except for an inevitable abrupt pressure change at the streamwise position of the cylinder. The main flow velocity was 14 m s^{-1} and its turbulent intensity level was within 1%.

The test section is shown in Fig. 2 together with the definition of the coordinates x and y, and of some geometric parameters H and d. The first part of the flat plate (from 10 to 200 mm downstream from the leading edge) was covered by a sand paper to trip the boundary layer. Heating of the surface started from a position 213 mm downstream from the leading edge. Thin metal (stainless steel) sheets of 50 μm thickness were glued on the surface of the flat plate made of bakelite. These sheets were heated by an alternating electric current. For measuring the streamwise distribution of the surface temperature, 90 alumel–chromel thermocouples of 0.1 mm diameter were attached to the back surface of a metal sheet glued along the center line of the flat plate. Twenty-two alumel–chromel thermocouples were also attached to the back

† The late Professor, Department of Mechanical Engineering, Setsunan University, Neyagawa, Osaka 572, Japan.

NOMENCLATURE

C_f	skin friction coefficient
d	diameter of the cylinder [mm]
H	distance between the cylinder axis and the flat plate [mm]
H'	hole size parameter for quadrant analysis
h	local heat transfer coefficient [$W m^{-2} K^{-1}$]
h_0	local heat transfer coefficient for undisturbed boundary layer [$W m^{-2} K^{-1}$]
I_i	indicator for quadrant analysis
St	Stanton number
U_e	free stream velocity [$m s^{-1}$]
u, u'	fluctuating component of streamwise velocity and its intensity [$m s^{-1}$]
u_τ	friction velocity [$m s^{-1}$]
$\overline{uv}$	turbulent shear stress [$m^2 s^{-2}$]
$\widetilde{uv}_i$	contribution to turbulent shear stress from the ith quadrant [$m^2 s^{-2}$]
v, v'	fluctuating component of normal velocity and its intensity [$m s^{-1}$]
$\overline{v\theta}$	turbulent heat flux [$m K s^{-1}$]
$\widetilde{v\theta}_i$	contribution to turbulent heat flux from the ith quadrant [$m K s^{-1}$]
x	streamwise distance measured from a cylinder [mm]
y	distance between the cylinder axis and the flat plate [mm].

Greek symbols

θ	fluctuating component of temperature [K]
θ_τ	friction temperature [K].

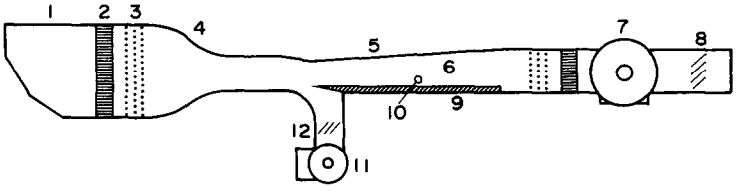

FIG. 1. Wind tunnel: 1, inlet to the tunnel; 2, honeycomb; 3, screen; 4, contraction chamber; 5, upper wall; 6, test section; 7, main suction type blower; 8, 12, flow rate controller; 9, flat plates; 10, cylinder; 11, blower.

surface of the bakelite plate. Assuming one-dimensional heat conduction, the temperature difference across the bakelite plate was used to calculate the rate of conductive heat loss through the back surface of the plate. For the calculation of radiative heat loss, the absorptivity of the metal sheet was assumed to be 0.2. The conductive and radiative heat transfer were subtracted from the electric heat generation rate to yield the net convective heat transfer rate. The local heat transfer coefficient was measured this way for the case when no cylinder was inserted and was found to agree well with an empirical equation given by Johnson and Rubesin [3] for a flat plate boundary layer. All the experiments were carried out for the heating condition of a wall heat flux of about 1 kW m^{-2}.

A cylindrical copper tube with 8 mm o.d. and 4 mm i.d. was used to disturb the boundary layer and was heated by circulating hot water through the inside. Four alumel–chromel thermocouples were attached to the upper, lower, front and back surface of the cylinder to check its temperature. The temperature difference between the cylinder surface and the flat plate surface just beneath the cylinder was kept to within ± 0.5 K. The cylinder was located at a streamwise position 1400 mm downstream from the leading edge flat plate. It was held detached from the flat plate in a position normal to the flow direction and parallel to the flat plate. Turbulence measurements were made downstream from the cylinder. When the cylinder was not inserted into the flow and

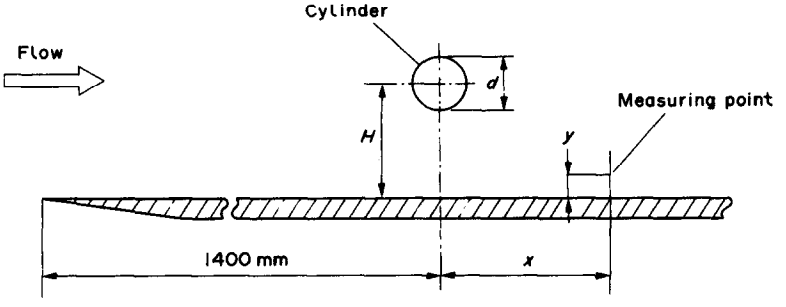

FIG. 2. Test section.

when the plate was unheated, the boundary layer thickness was about 28 mm at the cylinder insertion position. Measurements of the heat transfer coefficient were made for three cases of different distance between the cylinder axis and the flat plate H of 6, 15 and 33.5 mm. At these positions, detailed measurements of flow and turbulence characteristics had been previously obtained for the unheated cylinder [4–6]. Simultaneous measurements of streamwise and normal components of velocity fluctuations and of temperature fluctuation were carried out only in the case of $H = 15$ mm. The measurements were performed at five streamwise locations of $x = 37$, 87, 187, 387 and 837 mm along the center line of the flat plate.

The simultaneous measurements of streamwise and normal components of velocity fluctuation u and v and of temperature fluctuation θ were made with a combination of an X-type hot-wire and I-type cold-wire arrangement. The cold wire, used in a constant current mode, was located 0.6 mm upstream of the geometric center of the X-type hot-wire probe, which was operated in a constant temperature mode. Static calibration of this probe was made for velocity and temperature using an external heating method, i.e. by positioning the probe in a flow of controlled uniform velocity and temperature. Contamination of velocity signal caused by temperature fluctuation was removed later during data processing by making use of static calibration data. Distortion of the temperature signal caused by both the thermal inertia of the cold wire and the heat loss from the wire to the prongs was also corrected during data processing based on the static and dynamic calibration of the cold wire. The present calibration method is the same as that adopted in the previous study [2]. Each of the output signals from two constant temperature anemometers and a constant current bridge was digitized on line at the sampling rate of 10 kHz for each signal and recorded at about 20 s intervals for every measuring point on a magnetic disc connected to a PDP-11/23 minicomputer. Linearization and processing of the data were later done by a computer at the Kyoto University Data Processing Center.

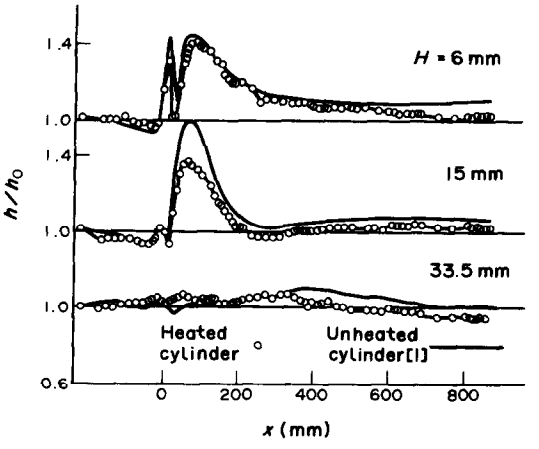

FIG. 3. Distribution of local heat transfer coefficient: (a) $H = 6$ mm; (b) $H = 15$ mm; (c) $H = 33.5$ mm.

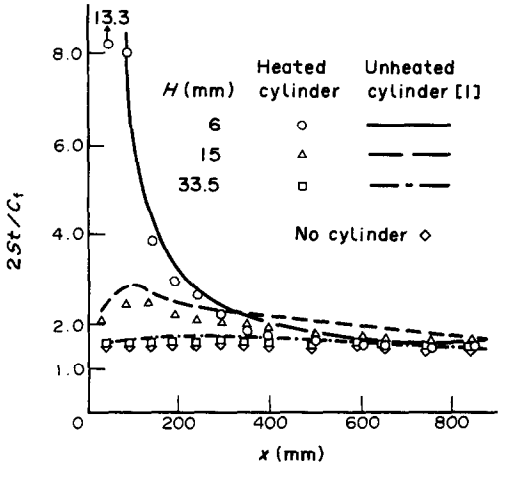

FIG. 4. Streamwise distribution of $2St/C_f$.

RESULTS AND DISCUSSION

Heat transfer coefficient

The distributions of the local heat transfer coefficient h along the flat plate are shown in Fig. 3 in the normalized form of h/h_0, where h_0 is the local heat transfer coefficient obtained at the same position for the case when no cylinder is inserted in the boundary layer. The x-axis of the figure denotes the streamwise distance measured downstream from the cylinder position.

Comparing the present results with the previous ones for the case with an unheated cylinder, the present heat transfer data are found to be slightly lower than the previous ones. Additionally, the shapes of the streamwise distribution of the local heat transfer coefficient are similar to each other. Therefore, it is clear that the heating of the cylinder does not significantly affect the heat transfer characteristics. For the present data, the ratio between the measured Stanton number St and half of the local skin friction coefficient $C_f/2$ is shown in Fig. 4. For the value of C_f, the data obtained by Marumo *et al.* [1] for an unheated boundary layer with a Pleston tube were used. This figure indicates that the ratio $2St/C_f$ is found to be very large in the region just downstream of the cylinder for both cases when $H = 6$ and 15 mm. This indicates that the dissimilarity between heat and momentum transfer exists just after the cylinder. In other words, even though the similarity in the boundary condition between the velocity and temperature fields is assured by heating the cylinder, heat transfer in the disturbed boundary layer does not obey the Reynolds analogy. Thus, the cause of the dissimilarity between heat and momentum transfer found in the present case is indicated to lie in the turbulence mechanism.

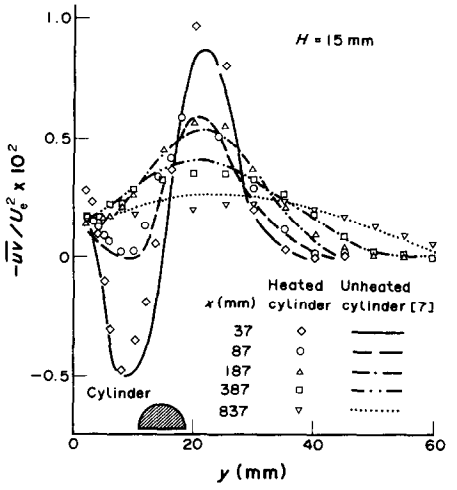

FIG. 5. Normal distribution of turbulent shear stress.

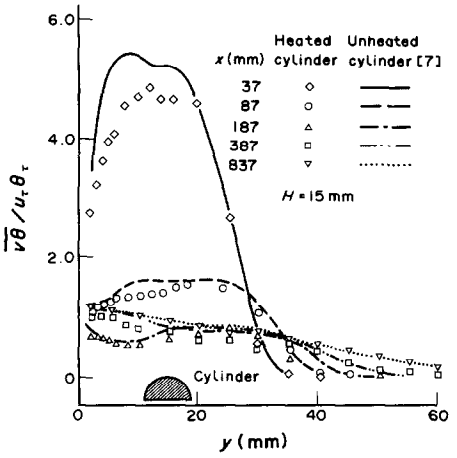

FIG. 6. Normal distribution of turbulent heat flux.

Turbulence characteristics

In order to discuss in more detail the dissimilarity between the heat and momentum transfer, simultaneous measurement of the streamwise and normal components of the velocity fluctuation u and v and of the temperature fluctuation θ was also made in the case when a heated cylinder was mounted at a normal position of $H = 15$ mm. An additional experiment was also performed for the case without a cylinder. The data of this additional experiment were used to check the accuracy of the present measurement of turbulence quantities in comparison with the results of Marumo *et al.* [1] and Kawaguchi *et al.* [2] for a case with an unheated cylinder.

In Fig. 5, the normal distribution of the measured value of Reynolds shear stress $-\overline{uv}$ is shown normalized with the free stream velocity U_e. The lines in the figure represent the previous results for the unheated cylinder [7]. No systematic deviation can be found between the present and previous results in Fig. 5. This is reasonable since the velocity field is only slightly affected by heating the cylinder. Almost the same conclusion can be drawn also for the statistical turbulence quantities associated with the temperature fluctuation. For example, the distribution of turbulent heat flux $\overline{v\theta}$ is shown in Fig. 6 normalized with the friction velocity u_τ and the friction temperature θ_τ. As shown in Fig. 6, the distribution of $\overline{v\theta}$ is most certainly affected by the heating of the cylinder, but the effect is small and limited only in the region of small x and between the cylinder and the flat plate. Therefore, it is again confirmed that the dissimilarity of boundary conditions between the velocity and temperature fields is not a major cause of the dissimilarity found between the heat and momentum transfer in this boundary layer.

Quadrant analysis

Lu and Willmarth [8] applied the u–v plane quadrant analysis to the instantaneously measured u and v signals. Especially for the purpose of analyzing the turbulent heat transfer mechanism, another method of conditional data analysis was introduced in the present study by taking into account the signs of u, v and θ. In order to classify the instantaneous fluid motions in the u–v–θ space, an indicator function I_i was defined as

$$I_i = \begin{cases} 1 \text{ (when the signs of } u, v \text{ and } \theta \text{ correspond to the } i\text{th quadrant of } u\text{–}v\text{–}\theta \text{ space and } |uv| > H'u'v') \\ 0 \text{ (otherwise)} \end{cases}$$

where H' is sometimes called the hole size parameter. By using this hole size parameter, I_i has the additional property of distinguishing fluid motions with large amplitude of the product uv from those having smaller amplitude.

Instantaneous fluid motions are classified into each of eight quadrants and identified with the symbols as follows:

1st quadrant ($u > 0, v > 0, \theta < 0$); cold outward interaction (●)
2nd quadrant ($u < 0, v > 0, \theta < 0$); cold ejection-like motion (▼)
3rd quadrant ($u < 0, v < 0, \theta < 0$); cold wallward interaction (■)
4th quadrant ($u > 0, v < 0, \theta < 0$); cold sweep-like motion (▲)
5th quadrant ($u > 0, v > 0, \theta > 0$); hot outward interaction (○)
6th quadrant ($u < 0, v > 0, \theta > 0$); hot ejection-like motion (▽)
7th quadrant ($u < 0, v < 0, \theta > 0$); hot wallward interaction (□)
8th quadrant ($u > 0, v < 0, \theta > 0$); hot sweep-like motion. (△)

Fluctuations classified in the 2nd, 4th, 6th and 8th quadrants contribute positively to $-\overline{uv}$ and those in the 1st, 3rd, 5th and 7th quadrants negatively to $-\overline{uv}$. Fluctuations in the 3rd, 4th, 5th and 6th quadrants contribute positively to $\overline{v\theta}$ and those in the 1st, 2nd, 7th and 8th quadrants negatively to $\overline{v\theta}$. Thus, for example, the cold sweep-like motion in the 4th quad-

rant and the hot ejection-like motion in the 6th quadrant always contribute positively to both the heat and momentum transfer. The cold outward interaction in the 1st quadrant and the hot wallward interaction in the 7th quadrant have negative contribution to both the heat and momentum transfer. All of these fluid motions contribute to both the heat and momentum transfer with the same sign. On the other hand, the fluid motions in the other four quadrants contribute to the heat and momentum transfer with opposite sign. For example, the hot outward interaction and cold wallward interaction discussed later in this paper contribute positively to the heat transfer but negatively to the momentum transfer. Therefore, they can incur dissimilar turbulent transport of heat and momentum.

The coherent fluid motion near the wall will be considered first. The conditional means of products uv and $v\theta$ are defined as

$$\widetilde{uv}_i = \overline{I_i uv}, \quad \widetilde{v\theta}_i = \overline{I_i v\theta}$$

where the overbar indicates an average over all the sampled data. By using the indicator I_i, strong fluid motions can be distinguished from weak ones. Since the conventional mean of $\overline{uv}$ or $\overline{v\theta}$ is the sum, respectively, of $\widetilde{uv}_i$ or $\widetilde{v\theta}_i$ for all possible values of i with $H = 0$, this classification makes it possible to determine which of the fluid motions specified above is the main contributor to the turbulent momentum and heat flux. For this purpose, attention is focused on the data obtained at a position closest to the flat plate where the normal position of the measuring point is 2 mm from the wall. In Fig. 7, some results of such an analysis are shown for the undisturbed case. The plotted values were normalized using the conventional mean of $\overline{uv}$ or $\overline{v\theta}$ at $u = 2$ mm. Figure 7 indicates that the hot ejection-like motion and the cold sweep-like motion dominate transport momentum and heat near the wall, and that the transport by the outward and wallward interactions are minor. The present results for the disturbed case with $H = 15$ mm for $X = 37$ and 87 mm are plotted in Fig. 8. Compared with the counterparts in the undisturbed case, the cold wallward interaction is found to be intensified by the effect of the disturbance given by the cylinder and its magnitude is approximately the same as that of the hot ejection-like motion or the cold sweep-like motion for any hole size. It is important to point out that the cold wallward interactions contribute negatively to $-\overline{uv}$ contrary to its positive contribution to $\overline{v\theta}$. A negative contribution to $-\overline{uv}$ leads to a smaller value of C_f while a positive contribution to $\overline{v\theta}$ suggests a higher value of St. This fact was also observed for the unheated cylinder [2]. Therefore, the difference in the boundary conditions between the temperature and velocity fields is not important and it is concluded that the cold wallward interaction is a fluid motion causing the dissimilarity between the heat and momentum transfer near the wall for the disturbed boundary layer.

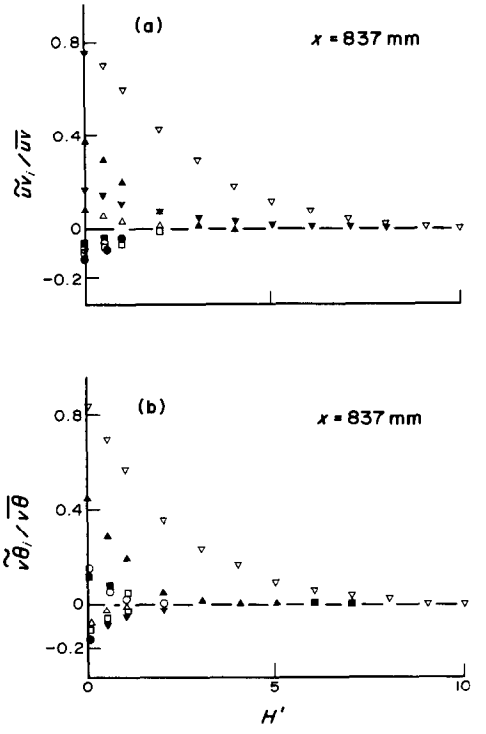

FIG. 7. Fractional contribution from the ith quadrant (undisturbed case; $y = 2$ mm): (a) to $\overline{uv}$; (b) to $\overline{v\theta}$.

One final consideration is how the contribution from each type of fluid motion to $\overline{uv}$ and $\overline{v\theta}$ is distributed throughout the boundary layer. The normal distributions of conditional means $\widetilde{uv}_i$ and $\widetilde{v\theta}_i$ obtained for each quadrant at $H' = 0$ are shown in Fig. 9 for the undisturbed case and in Fig. 10 for the disturbed case at a position of $x = 37$ mm. The plotted data are normalized with the conventional mean $\overline{uv}$ or $\overline{v\theta}$ at $y = 2$ mm. For the undisturbed case, only the hot ejection-like motion and the cold sweep-like motion are found to be major contributors to both $-\overline{uv}$ and $\overline{v\theta}$ at all measured points and the shapes of the distributions of $\widetilde{uv}_i$ and $\widetilde{v\theta}_i$ are found to be similar to each other. On the other hand, Fig. 10 shows the difference in the shapes among the distributions of $\widetilde{uv}_i$ and of $\widetilde{v\theta}_i$. Among others, the intensification of the cold wallward and hot outward interactions is noticeable. These interactions contribute negatively to $-\overline{uv}$ but positively to $\overline{v\theta}$. Thus, it can be concluded that the intensification of the hot outward and cold wallward interactions is a major cause of the dissimilarity existing between the heat and momentum transfer in the entire region of the boundary layer disturbed by a cylinder. This is the same as the suggestion previously drawn for the unheated cylinder [2]. Therefore, the heating of the cylinder is not important. Thus, it is concluded that the dissimilarity between heat and momentum transfer discussed in this paper is a feature intrinsic to the turbulence in the disturbed boundary layer.

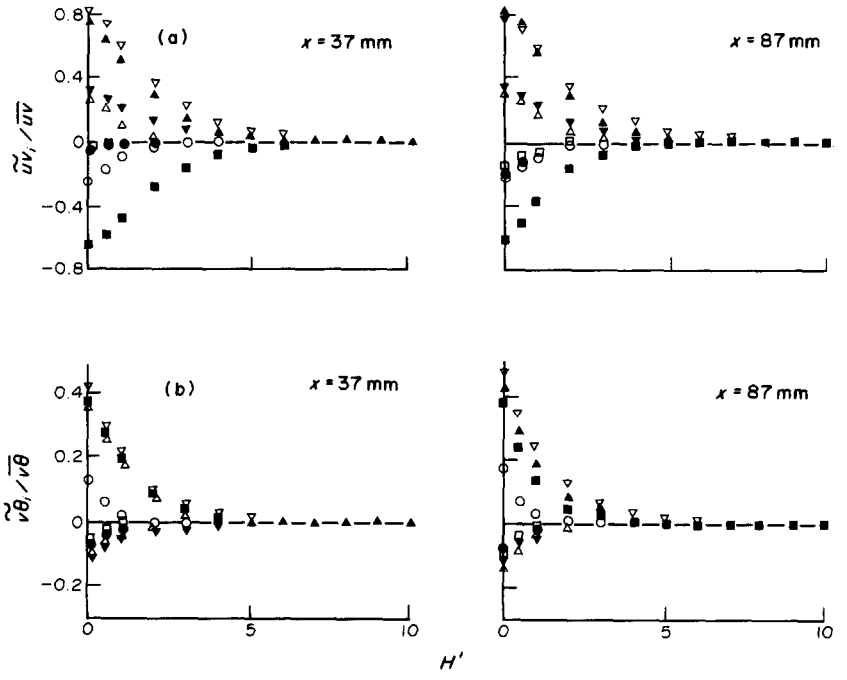

FIG. 8. Fractional contribution from the ith quadrant (disturbed case; $y = 2$ mm): (a) to $\overline{uw}$; (b) to $\overline{v\theta}$.

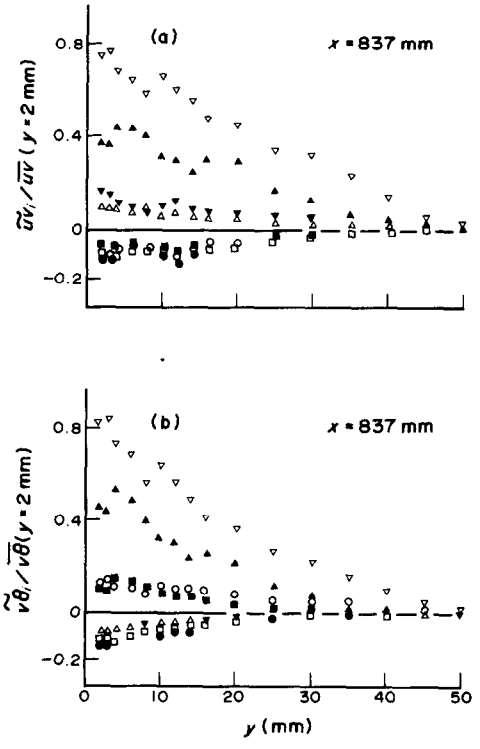

FIG. 9. Normal distribution of fractional contribution from the ith quadrant (undisturbed case): (a) to $\overline{uw}$; (b) to $\overline{v\theta}$.

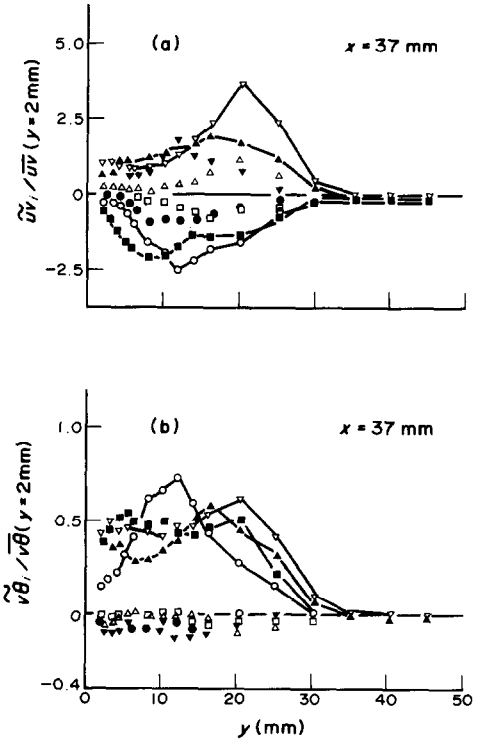

FIG. 10. Normal distribution of fractional contribution from the ith quadrant (disturbed case): (a) to $\overline{uw}$; (b) to $\overline{v\theta}$.

CONCLUSIONS

This paper dealt with a boundary layer disturbed by a cylinder. Dissimilarity between heat and momentum transfer was previously found for the cases with an unheated cylinder. The particular purpose of this study was to determine if such a dissimilarity is due to the difference between the boundary conditions for the velocity and temperature fields caused by the unheated cylinder, or if it is an intrinsic feature of the turbulence in the disturbed boundary layer. For this purpose, experiments were carried out by heating the cylinder to the same temperature as the flat plate. The distribution of the heat transfer coefficient indicated that the dissimilarity between heat and momentum transfer exists even for the heated cylinder. The heat transfer coefficient was reduced by the heating of the cylinder but its change was rather small. Thus, the dissimilarity in the boundary condition between the velocity and temperature field was not an important factor causing the dissimilarity between heat and momentum transfer.

For a detailed discussion on the dissimilarity, simultaneous measurements of u, v and θ were made. The normal distribution of the turbulent shear stress $-\overline{uv}$ connected to the momentum transfer was affected little by heating the cylinder. The normal distribution of the turbulent heat flux $\overline{v\theta}$ associated with heat transfer was affected in the near wall region at cross-sections close to the cylinder but the effect was again small.

At the position closest to the wall, $x = 37$ mm, intensification of the cold wallward interaction was found to be a major factor causing dissimilarity between heat and momentum transfer. In the entire region of the boundary layer, the intensification of the cold wallward and hot outward interactions were found and concluded to be major fluid motions causing the dissimilarity between heat and momentum transfer in the present disturbed boundary layer.

REFERENCES

1. E. Marumo, K. Suzuki and T. Sato, Turbulent heat transfer in a flat plate boundary layer disturbed by a cylinder, *Int. J. Heat Fluid Flow* **6**, 241–248 (1985).
2. Y. Kawaguchi, Y. Matsumori and K. Suzuki, Structural study of momentum and heat transport in the near wall region of a disturbed boundary layer, 9th Biennial Symposium on Turbulence (1984).
3. H. A. Johnson and M. W. Rubesin, Aerodynamic heating and convection heat transfer—summary of literature survey, *Trans. ASME* **71**, 447–456 (1939).
4. E. Marumo, K. Suzuki and T. Sato, A turbulent boundary layer disturbed by a cylinder, *J. Fluid Mech.* **87**(1), 121–141 (1978).
5. E. Marumo, K. Suzuki, T. Sasaki and T. Sato, A turbulent boundary layer disturbed by a cylinder (1st report), *Trans. JSME* **46**(407), 1211–1219 (1980).
6. E. Marumo, K. Suzuki, T. Sasaki, H. Kinuta and T. Sato, A turbulent boundary layer disturbed by a cylinder (2nd report), *Trans. JSME* **46**(407), 1220–1228 (1980).
7. T. Yano, Y. Kawaguchi and K. Suzuki, Large-scale motion in the region of a turbulent boundary layer disturbed by a cylinder, 22nd National Heat Transfer Symposium in Japan, pp. 154–156 (1985).
8. S. S. Lu and W. W. Willmarth, Measurements of the structure of the Reynolds stress in a turbulent boundary layer, *J. Fluid Mech.* **60**(3), 481–511 (1973).

DIFFERENCE ENTRE LES TRANSFERTS DE CHALEUR ET DE QUANTITE DE MOUVEMENT DANS UNE COUCHE LIMITE TURBULENTE PERTURBEE PAR UN CYLINDRE

Résumé—On étudie, du point de vue de la structure turbulente, la cause de la différence entre les transferts de chaleur et de quantité de mouvement observée dans la couche limite d'une plaque plane, perturbée par un cylindre. On en déduit que l'intensification des intéractions entre la zone externe chaude et la zone froide pariétale induites par la perturbation créée par le cylindre est la cause principale de la différence remarquée.

UNTERSCHIED ZWISCHEN DER WÄRME- UND IMPULSÜBERTRAGUNG IN EINER TURBULENTEN, DURCH EINEN ZYLINDER GESTÖRTEN GRENZSCHICHT

Zusammenfassung—Die Ursache für die fehlende Ähnlichkeit zwischen Wärme- und Impulstransport, welche sich in der von einem Zylinder gestörten Grenzschicht einer ebenen Platte zeigt, wurde im Hinblick auf die Turbulenzstruktur untersucht. Es ergibt sich, daß die Verstärkung der Wechselwirkungen zwischen der heißen äußeren und der kalten Wand-Seite, die infolge der Störung durch den Zylinder entstehen, eine Hauptursache für das Fehlen der Ähnlichkeit ist.

НАРУШЕНИЕ ПОДОБИЯ МЕЖДУ ПЕРЕНОСОМ ТЕПЛА И ИМПУЛЬСА В ТУРБУЛЕНТНОМ ПОГРАНИЧНОМ СЛОЕ ВОЗМУЩЕНИЯМИ, ВЫЗВАННЫМИ ОБТЕКАНИЕМ ЦИЛИНДРА

Аннотация—Причина нарушения подобия между переносом тепла и импульса в пограничном слое на плоской пластине возмущениями, вызванными обтеканием цилиндрической поверхности, рассматривается с точки зрения турбулентных структур. Сделан вывод о том, что интенсификация горячих по отношению к внешней границе и холодных по направлению к стенке взаимодействий, инициированная возмущениями, внесенными цилиндром, является основной причиной нарушения подобия.